silver electrodes from which photoelectron ejection at 0 V occurs with a quantum yield below 10^{-4}.[20] However, quasi-metallic particles (broad plasmon absorption band around 360 nm) still eject an electron upon illumination although the quantum yield of 0.007 is clearly lower than for the nonmetallic clusters. We thus see a gradually changing ability to photoeject an electron with decreasing size of silver particles in the transition range from bulk material to atoms.

The photofragmentation of almost metallic particles to yield small clusters (Figure 11) is possibly also an event following ejection of an electron. However, further experiments are required to investigate this question in more detail.

(20) Sass, J. K.; Sen, R. K.; Meyer, E.; Gerischer, H. *Surf. Sci.* **1974**, *44*, 515.

Registry No. $AgClO_4$, 7783-93-9; $NaBH_4$, 16940-66-2; Ag^+, 14701-21-4; Ag, 7440-22-4; CH_3OH, 67-56-1; O_2, 7782-44-7; H_2O_2, 7722-84-1; *tert*-butyl alcohol, 75-65-0.

Picosecond Time-Resolved Resonance Raman Scattering and Absorbance Changes of Carotenoids in Light-Harvesting Systems of Photosynthetic Bacterium *Chromatium vinosum*

H. Hayashi,‡ S. V. Kolaczkowski, T. Noguchi, D. Blanchard, and G. H. Atkinson*,†

Contribution from the Department of Chemistry and Optical Science Center, University of Arizona, Tucson, Arizona 85721. *Received February 7, 1989*

Abstract: The excited electronic states of carotenoids in light-harvesting systems of photosynthetic bacteria are examined by picosecond laser spectroscopy. Picosecond changes in absorbance and in the intensity of resonance Raman bands are observed for carotenoids (mainly rhodopin and spirilloxanthin) in *Chromatium vinosum*. These data are obtained with picosecond transient absorption and picosecond time-resolved resonance Raman spectroscopies utilizing a two laser (8 ps pulses), pump-probe instrumental configuration. Following 560 nm pump laser excitation, sample absorbance between 573 and 650 nm initially increases and subsequently decays with a fast (6 ± 0.5 ps) and two slow (~80 ps and >200 ns) components. The initial rise and the fastest decay component reflect, respectively, the formation and relaxation of the excited 2^1A_g state of the carotenoids. The slow decay constants both reflect the decay of excited triplet state carotenoids although the 80-ps component remains to be fully characterized. The intensities of the RR bands assignable to the ground 1^1A_g state of the carotenoids decrease by more than 30% during the laser excitation and then increase with a rate of 6 ps, reflecting the depletion of the 1^1A_g state followed by its repopulation due to the relaxation of the 2^1A_g state. The transient populations of excited triplet states in carotenoids are observed through picosecond time-resolved resonance Raman spectra containing several new resonance Raman bands, at 1475, 1260, 1171, 1124, and 1007 cm^{-1}.

In photosynthetic bacteria, light energy absorbed by carotenoids and bacteriochlorophylls (BChls) located in the light-harvesting pigment–protein complexes is transferred to photosynthetic reaction centers.[1,2] This light-harvesting function of the carotenoid is critical to the efficient utilization of light energy in the primary charge separation reaction. In addition, carotenoids in both the light-harvesting complexes and reaction centers protect BChls from photochemical damage caused by light and oxygen.[3] The participation of electronically excited states, such as the first excited singlet and triplet states, of the carotenoids are fundamental to both types of processes. Accordingly, a detailed understanding of the light-harvesting and photoprotective processes requires detailed investigations of the rates of these processes and the molecular vibrations that underlie them in electronically excited-state carotenoids.

Excited-state carotenoids, in both in vitro and in vivo preparations, have been examined by transient absorption and resonance Raman (RR) spectroscopies in a variety of previous studies.[4-21] Of importance here is that the main optical transition (near 480 nm in β-carotene and 520 nm in chromatophores from *Chromatium vinosum*) from the ground 1^1A_g (S_0) state populates the excited 1^1B_u state. The 1^1B_u state rapidly crosses to the excited 2^1A_g state, which lies energetically nearby. The 2^1A_g state is populated only from the 1^1B_u state since the $1^1A_g \rightarrow 2^1A_g$ optical transition is formally forbidden, with an indirectly estimated rate constant of $< 1 \times 10^{12}$ s^{-1}.[15,16] The 2^1A_g state of in vitro β-carotene decays to the ground state in 8.4 ps as observed by ground-state

* To whom correspondence should be addressed.
† Senior Alexander von Humboldt Awardee.
‡ Permanent address: Department of Chemistry, Faculty of Science, The University of Tokyo, Hongo, Tokyo 113, Japan.

(1) van Grondelle, R.; Amesz, J. *Light Emission by Plants and Bacteria*; Govinjee, Amesz, J., Fork, D. C. Eds.; Academic Press: New York, 1986; pp 191-223.
(2) Siefermann-Harms, D. *Biochim. Biophys. Acta* **1985**, *811*, 325-355, and references therein.
(3) Cohen-Bazier, G.; Stainier, R. Y. *Nature* **1958**, *181*, 250-252.
(4) Cogdell, R. J.; Monger, T. G.; Parson, W. W. *Biochim. Biophys. Acta* **1975**, *408*, 189-199.
(5) Monger, T. G.; Cogdell, R. J.; Parson, W. W. *Biochim. Biophys. Acta* **1976**, *449*, 136-153.
(6) Truscott, T. G.; Land, E. J.; Sykes, A. *Photochem. Photobiol.* **1973**, *17*, 43-51.
(7) Bensasson, R.; Land, E. J.; Maudinas, B. *Photochem. Photobiol.* **1976**, *23*, 189-193.
(8) Cogdell, R. J.; Land, E. J.; Truscott, T. G. *Photochem. Photobiol.* **1983**, *38*, 723-725.
(9) Thrash, R. J.; Fang, H. L. B.; Leroi, G. E. *J. Chem. Phys.* **1977**, *67*, 5930.
(10) Thrash, R. J.; Fang, H. L.-B.; Leroi, G. E. *Photochem. Photobiol.* **1979**, *29*, 1049.
(11) Jensen, N.-H.; Wilbrandt, R.; Pagsberg, P. B.; Sillesen, A. H.; Hansen, K. B. *J. Am. Chem. Soc.* **1980**, *102*, 7441-7444.
(12) Dallinger, R. F.; Farquharson, S.; Woodruff, W. H.; Rodgers, M. A. J. *J. Am. Chem. Soc.* **1981**, *103*, 7433-7440.
(13) Dallinger, R. F.; Woodruff, W. H.; Rodgers, M. A. J. *Photochem. Photobiol.* **1981**, *33*, 275-277.
(14) Lutz, M.; Chinsky, L.; Turpin, P.-Y. *Photochem. Photobiol.* **1982**, *36*, 503-515.
(15) Haley, L. V.; Koningstein, J. A. *Chem. Phys.* **1983**, *77*, 1-9.
(16) Wylie, I. W.; Kongingstein, J. A. *J. Phys. Chem.* **1984**, *88*, 2950-2953.
(17) Nuijs, A. M.; van Grondelle, R.; Joppe, H. L. P.; van Bochove, A. C.; Duysens, L. N. M. *Biochim. Biophys. Acta* **1985**, *810*, 94-105.

0002-7863/90/1512-4664$02.50/0

repopulation.[18,19] The carotenoid, spheroidene, present in the B800-850 (or light-harvesting II) antenna complex of *Rhodobacter acidophila* transfers energy to the 850 nm absorbing BChl *a* dimer in 6.1 ± 0.9 ps.[20] These data indicate that it is the longer lived 2^1A_g state which participates in singlet energy transfer and the other photochemical processes. The energies and relative energy positions of the 1^1B_u and 1^1A_g states change as a function of molecular (polyene) length with the state being at lower energy for polyenes longer than heptaenes.[22,23] This state ordering also is generally assumed to be correct for carotenoids.

In light-harvesting complexes, triplet state carotenoids are formed via either triplet–triplet energy transfer, from either triplet state bacteriochlorophyll or singlet oxygen, or by singlet fission of the 2^1A_g state in combination with a second ground-state carotenoid.[24-27] The singlet fisson process results in the formation of two triplet state (T_1) carotenoids in close proximity to each other. The excited triplet state of carotenoids has a lifetime of about 1 μs and an intense $T_1 \rightarrow T_n$ absorption transition centered near 560 nm in in vivo preparations. In in vivo preparations, the intensity of the $T_1 \rightarrow T_n$ transition is approximately 2–3 times more intense than the singlet $1^1A_g \rightarrow 1^1B_u$ transition.[4,17]

Previously, absorption from the excited singlet states (either 1^1B_u or 2^1A_g) has been reported for carotenoids in chromatophores from *Rhodospirillum rubrum*.[17] Given the laser powers and the time resolution in these experiments, 35 ps, it was not possible to assign the transition to a specific excited singlet state (1^1B_u or 2^1A_g) or to clearly separate the absorbance contributions of the excited-triplet state.[17] Consequently, the rates of decay of the 2^1A_g state to form either ground-state or triplet-state carotenoid could not be determined.

For structural studies of in vivo carotenoids, RR spectroscopy is one of the most powerful spectroscopic techniques currently available. RR spectra of T_1 states have been observed for several species of isolated carotenoids (in organic solvents) by using a time-resolved pulse radiolysis and photolysis.[11,12,14,20] RR spectra of the T_1 state carotenoids in bacterial photosynthetic reaction centers also have been reported.[14] Recently, RR spectra of the excited S_1 state have been reported for extracted β-carotene[28,29] after several unsuccessful attempts to record these data by using transient Raman measurements with single pulsed laser excitation.[13,15,16] However, neither the T_1 state nor the S_1 state of carotenoids in the light-harvesting systems of photosynthetic organisms have been observed by RR spectroscopy.

In this study, the excited electronic states of carotenoids (mainly spirilloxanthin and rhodopin) in the in vivo chromatophores of *Ch. vinosum* are examined. Picosecond time-resolved resonance Raman (PTR³) spectroscopy is utilized to record the RR spectra of the excited triplet state (T_1) and the transient ground-state (1^1A_g) population. Picosecond transient absorption (PTA) spectroscopy is used to measure the corresponding absorbance changes from the T_1 and the 2^1A_g excited states. Both types of measurements clearly reveal the formation and relaxation of excited states and the depletion and repopulation of the ground states of the carotenoids. Since both the pump and probe lasers have 8-ps pulses, absorbance changes assignable to the 2^1A_g state can be clearly identified and separated from the absorbance change due to the T_1 state. Furthermore, the RR spectrum of the T_1 state of carotenoids in an in vivo light-harvesting system is reported here for the first time.

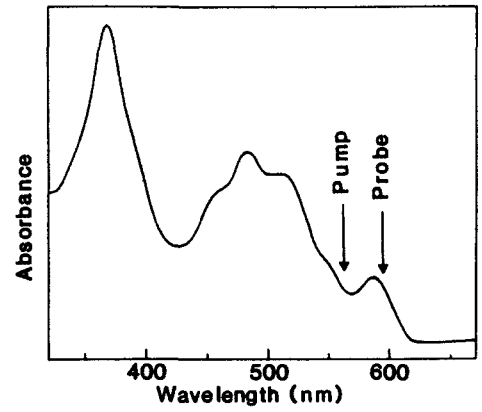

Figure 1. Absorption spectrum of chromatophores from *Chromatium vinosum* in the 330–670-nm region. For the measurement of the absorption spectrum, a sample for PTA and PTR³ measurements is diluted to 1/20 with Tris buffer to adjust the OD_{590} to 0.25. The PTA and PTR³ measurements are recorded for a sample with an OD_{590} of 5 at room temperature. Two arrows indicate the position of the pump laser and the probe laser for the PTR³ measurement.

Experimental Section

The intracytoplasmic membranes (chromatophores) are prepared from *Chromatium vinosum* and *Rhodobacter sphaeroides* (carotenoid-less mutant) as reported previously[30] and suspended in a 50 mM Tris buffer (pH 8.4) to give a sample absorbance of 5 at 590 nm with a 10-mm light path. The sample suspension is circulated by a mechanical pump (Micropump, Model 8051) through a 300 ± 50 μm (ID) glass nozzle. The sample reservoir and pump head are immersed in ice and water to maintain the sample at a constant temperature of 12 °C. The velocity of the sample jet is fast enough (20 m/s) to prevent two successive pairs of laser pulses from illuminating the same volume when the pump and probe laser systems are both operated at 1 MHz repetition rates.

The instrumentation is described in detail elsewhere.[31-34] Briefly, two dye lasers (Coherent Model 702-3) are synchronously pumped by the second harmonic frequency of a mode-locked Nd:YAG laser (Quantronix Model 416 and SHG Model 324) to produce 8-ps (FWHM) pulses at 1-MHz repetition rates from each. One dye laser (560–565 nm, 10–15 mW) is used as a pump for the excitation of carotenoids, and the other (573–650 nm, 2–4 mW) is used as a probe laser for the measurement of the absorbance changes and to generate RR scattering. The pump and probe laser beams are aligned collinearly before being focused into the liquid jet with a microscope objective. The illuminated sample is contained within an 18 μm diameter volume. The picosecond delay times between the pump and probe laser pulses are obtained with an optical delay line.

For the measurement of absorbance changes, the collinear probe and pump laser beams are separated by a prism after passing through the sample jet. The intensity of the probe laser (573–650 nm) is monitored by a photodiode operating in conjunction with a lock-in amplifier. The pump laser beam is chopped mechanically at about 500 Hz to provide the trigger pulse needed for the phase-sensitive detection of intensity changes in the probe laser.

To record PTR³ data, the pump and probe laser are operated without chopping either beam. The RR scattering is collected at 90° to the plane formed by the sample jet and the two laser beams. A triple monochro-

(18) Wasielewski, M. R.; Liddell, P. A.; Barrett, D.; Moore, T. A.; Gust, D. *Nature* **1986**, *322*, 570–572.
(19) Wasielewski, M. R.; Kispert, L. D. *Chem. Phys. Lett.* **1986**, *128*, 238–243.
(20) Wasielewski, M. R.; Tiede, D. M.; Frank, H. A. In *Ultrafast Phenomena V*; Fleming, G. R., Siegman, A. E., Eds.; Springer-Verlag: 1986; Vol. 46, pp 388–392.
(21) Hashimoto, H.; Koyama, Y. *J. Phys. Chem.* **1988**, *92*, 2101–2108.
(22) Synder, R.; Arvidson, E.; Foote, C.; Harrigen, L.; Christensen, R. L. *J. Am. Chem. Soc.* **1985**, *107*, 4117–4122.
(23) Hudson, B. S.; Kohler, B. E.; Schulten, K. In *Excited States*; Lim, E. C., Ed.; Academic Press: New York, Vol. 6, pp 1–95.
(24) Rademaker, H.; Hoff, A. J.; van Grondelle, R.; Duysens, L. N. M. *Biochim. Biophys. Acta* **1980**, *592*, 240–257.
(25) Frank, H.; McGann, W. J.; Macknicki, J.; Felber, M. *Biochem. Biophys. Res. Commun.* **1982**, *106*, 1310–1317.
(26) Kingma, H.; van Grondelle, R.; Duysens, L. N. M. *Biochim. Biophys. Acta* **1985**, *808*, 363–382.
(27) Kingma, H.; van Grondelle, R.; Duysens, L. N. M. *Biochim. Biophys. Acta* **1985**, *808*, 383–401.
(28) Hashimato, H.; Koyama, Y. *Chem. Phys. Lett.* **1989**, *154*, 321–325.
(29) Noguchi, T.; Kolaczkowski, S.; Arbour, C.; Aramaki, S.; Atkinson, G. H.; Hayashi, H.; Tasumi, M. *Photochem. Photobiol.* **1989**, *50*, 603–609.
(30) Hayashi, H.; Morita, S. *J. Biochem.* **1980**, *88*, 1251–1258.
(31) Atkinson, G. H.; Brack, T. L.; Blanchard, D.; Rumbles, G.; Siemankowski, L. In *Ultrafast Phenomena V*; Fleming, G. R.; Siegman, A. E., Eds.; Springer-Verlag: New York, 1986; Vol. 46, p 409.
(32) Atkinson, G. H. In *Primary Processes in Photobiology*; Kobayashi, T., Ed.; Springer Verlag: New York, 1987; pp 213–222.
(33) Atkinson, G. H.; Blanchard, D.; Lemaire, H.; Brack, T.; Hayashi, H. Biophys. *J.* **1989**, *55*, 263–274.
(34) Atkinson, G. H.; Brack, T.; Blanchard, D.; Rumbles, G. *Chem. Phys.* **1989**, *131*, 1–15.

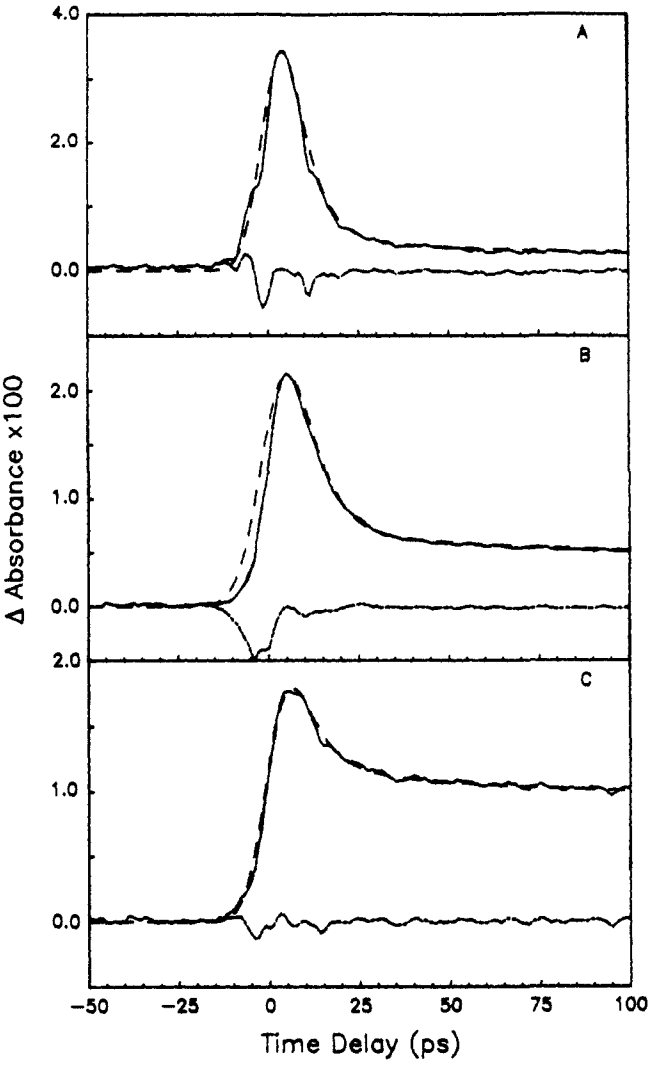

Figure 2. Time dependence of the absorbance changes at 582 (A), 590 (B), and 610 nm (C) of carotenoids in chromatophores from *Chromatium vinosum*. In each panel, the data are represented by the solid line, and the dashed line is the fit to the data (each fit is the convolution of the 8-ps pump and probe pulses with a 14-ps cross-correlation time with two decay functions of the form $A \exp(-kt)$ and a constant offset to model the long time absorbance change). The chain dashed line represents the difference between the data and the fit or residuals at each time point.

mator (Spex Triplemate) is used to disperse the RR scattering prior to detection by an intensified reticon array (EG&G, Model 1463). The reticon signal is processed by an optical multichannel analyzer prior to being transferred to a computer for data storage and analysis. Contributions from the pump laser are subtracted to obtain the RR spectrum of the mixture of species present at a given time delay.

Results

An absorption spectrum of chromatophores from *Ch. vinosum* in the visible region is shown in Figure 1. The absorption maxima at 370 and 590 nm, respectively, correspond to Soret and Q_x bands of bacteriochlorophyll *a* (BChl), while those between 400 and 550 nm arise from the carotenoids (mainly rhodopin and spirilloxanthin). Arrows indicate positions of the pump (565 nm) and probe (595 nm) lasers used for the PTR[3] measurements.

The time dependence of absorbance changes at three wavelengths (582 nm, 590 nm, and 610 nm) are shown in Figure 2 for time delays ranging from −50 ps (i.e., the probe pulse occurring 50 ps before the pump pulse) to 100 ps. The 0-ps delay corresponds to the temporal overlap of the pump and probe laser pulses as measured by the cross-correlation. The pump and probe laser pulses each have autocorrelation pulse widths of 12 ps and a cross-correlation pulse width of 14 ps. The autocorrelation measurements demonstrate that for a Gaussian approximation

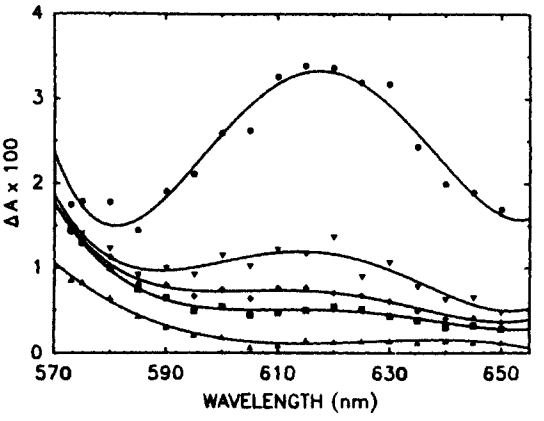

Figure 3. Changes in absorbance of carotenoids in chromatophores from *Ch. vinosum* at specific time delays [0 ps (●), 8 ps (▼), 12 ps (◆), 18 ps (■), and 400 ps (▲)] are plotted versus the probe laser wavelength. These data points are fitted to a sixth order polynominal function. Experimental conditions remain the same as those described in the text.

to the pulse shape, each laser produces pulses of 8-ps duration (FWHM). The cross-correlation and the auto-correlation measurements indicate a small timing jitter (~7 ps[35]) exists in the optical alignment used to temporally overlap the two laser pulses. The increase in absorbance observed at a 0-ps delay correlates directly with the cross-correlation characteristics of the pump and probe pulses.

According to standard methods,[36] the absorbance decays are deconvoluted with at least three components. The fastest decay constant is 6.0 ± 0.5 ps, while the two slower constants are approximately 80 ps and > 200 ns, respectively. The fastest rate is determined by deconvoluting the cross-correlation from the PTA data. The 80-ps component can only be approximated due to instrumental limitations of the optical delay line. The absorbance remaining after 100-ps decays with the same decay constant as the recovery of the intensities in the ground-state carotenoid Raman bands, vide infra. The decay constants are the same for all of the probe wavelengths measured, but the relative contributions of each decay process varies greatly as a function of wavelength. At 582 nm, for example, the contribution of the 6-ps component is comparable to that of the slower components, while at 610 nm the contribution of the 6-ps component is dominant.

The absorption spectra of the excited-state intermediates can be obtained by plotting the absorbance changes at given time delays as a function of probe laser wavelength. These absorbance changes, recorded 0, 12, 18, 25, and 400 ps after pump-laser excitation, are presented in Figure 3. The 0-ps data contain an intensity maximum at about 620 nm. No well-defined intensity maximum appears in the 573–650-nm region for the 18–400-ps data although it is clear that an intensity maximum is present at wavelengths shorter than 570 nm. It also is evident that the species absorbing at wavelengths less than 570 nm has a longer lifetime than the species with an absorption maximum at 620 nm. In addition, it can be noted from a comparison of the 18- and 25-ps data with those obtained from the 400-ps delay that the absorbance decreases uniformly throughout the 573–650-nm region.

The RR spectrum measured with a single, low-energy (4 mW) laser operating at 595 nm (i.e., probe laser only without the 565-nm pump laser excitation) is presented in Figure 4A. Since the 595-nm excitation wavelength is almost the same as the absorption maximum of BChl (Q_x band, Figure 1), a large resonance enhancement of the Raman scattering from BChl is to be expected. However, only the moderate to weak intensity bands appearing at 1610 and 1337 cm^{-1} can be assigned to BChl. These features correspond well with the RR bands of in vitro BChl previously reported from a study by using CW laser excitation around 590

(35) Clemens, J. M.; Najbar, J.; Bronstein-Bonte, I.; Hochstrasser, R. M. *Optics Commun.* **1983**, *47*, 271.
(36) Jansson, P. A. *Deconvolution with Applications in Spectroscopy*; Academic Press Inc.: New York, 1984.

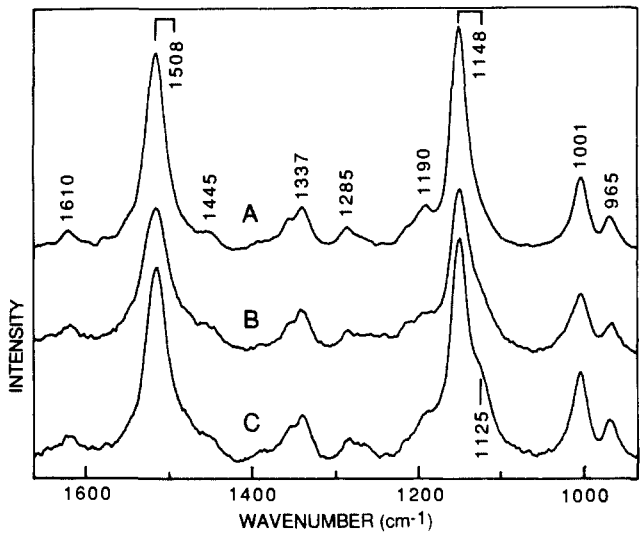

Figure 4. Resonance Raman (RR) and picosecond time-resolved resonance Raman (PTR^3) spectra of pigments in chromatophores from *Ch. vinosum*. (A) RR spectrum of ground-state carotenoids measured by 595-nm probe laser only (8 ps, 4 mW, 1 MHz), (B) PTR^3 spectrum measured with a 0-ps delay of 595 nm probe laser pulse (as described in (A)) after pumping by 565-nm pulse (8 ps, 15 mW, 1 MHz), and (C) PTR^3 spectrum measured with the same conditions as described in (B) except with a 50-ps delay. For PTR^3 data (B and C), emission due to the pump laser is measured separately and subtracted to obtain spectra presented. All three spectra are normalized to the wavelength dependence of the detector sensitivity. The wavenumber displacement from probe laser is calibrated with neon lines. See text for assignments of RR bands.

nm.[37] By contrast, two strong bands at 1508 and 1148 cm^{-1} and several weak bands at 1445, 1285, 1190, 1001, and 965 cm^{-1} are attributable to RR scattering from ground-state carotenoids. All of these latter RR features correlate closely to structure observed in the RR spectra of ground-state carotenoids measured under rigorously resonant conditions (e.g., with a CW laser operating at 488 nm[38,39]). The RR bands of carotenoids, therefore, dominate the spectrum presented in Figure 4A, while RR scattering assignable to BChl makes only a minor contribution.

The PTR^3 spectrum observed with the probe laser operating at 595 nm and 0-ps delay is presented in Figure 4B. Clearly, the relative intensities of RR bands assignable to ground-state carotenoids at 1508 and 1148 cm^{-1} are significantly smaller than those observed in the probe laser only spectrum (Figure 4A). In addition, (i) a shoulder around 1125 cm^{-1} appears, (ii) the RR scattering near 1170 cm^{-1} increases (most easily recognized in Figure 4B through the disappearance of the intensity minimum between the 1190- and 1148-cm^{-1} bands seen in Figure 4A), and (iii) the 1508-cm^{-1} band broadens to both higher and lower energies. The same comparison of spectra (Figure 4A and 4B) demonstrates that the relative intensities and positions of the RR bands attributable to BChl (1610 and 1337 cm^{-1}) remain unchanged. The PTR^3 spectrum observed 50 ps after the pump laser excitation (Figure 4C) has many of the same features as those found in the probe laser only spectrum (Figure 4A). For example, the ground-state carotenoid bands at 1508 and 1148 cm^{-1} have almost regained the intensities found in the probe only spectrum (Figure 4A). There are, however, several significant differences. The shoulder at 1125 cm^{-1} is clearly observable at a 50-ps delay, while the increased intensity near 1170 cm^{-1} has formed a distinct shoulder which obscures any feature that may remain at 1190 cm^{-1}. Similarly, a shoulder on the low-energy side of the 1508-cm^{-1} band appears. The differences between the probe laser only spectrum and the two PTR^3 spectra (0- and 50-ps delay) are more evident in the difference spectra presented in Figure 5 vide infra.

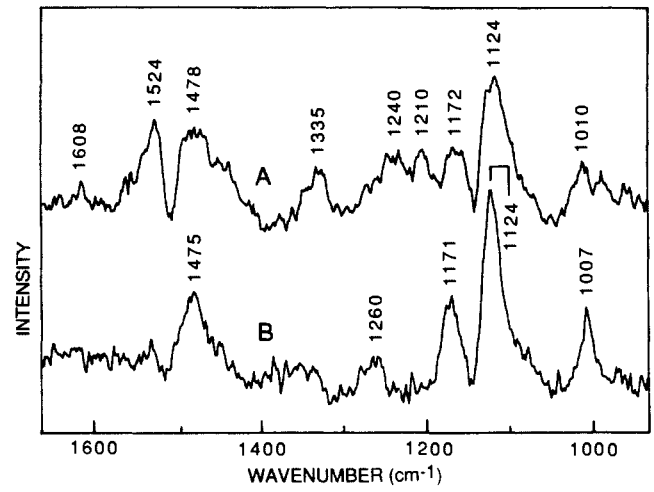

Figure 5. RR spectra of the excited triplet state carotenoids in chromatophores of *Ch. vinosum*. (A) RR spectrum obtained by subtracting 70% of probe laser only spectrum (Figure 4A) from PTR^3 data recorded with 0-ps delay (Figure 4B). (B) RR spectrum obtained by subtracting 98% of probe laser only spectrum (Figure 4A) from PTR^3 data recorded with 50-ps delay (Figure 4C). Bands at 1475, 1260, 1171, 1124, and 1007 cm^{-1} are assigned to the excited triplet state of the carotenoids. See text for discussion of scaling factors and assignments for RR bands.

Difference RR spectra, obtained by subtracting the probe laser only spectrum (Figure 4A) from a specific PTR^3 spectrum, are presented in Figure 5. Since the distribution of populations in the ground- and excited-states vary significantly at each time delay, the probe laser only RR spectrum must be scaled to accurately account for the ground-state RR scattering present in a given PTR^3 spectrum. The criteria used to derive the scaling factors are described in the discussion section. The difference RR spectrum obtained by subtracting 0.98 times the probe laser only RR spectrum from the 50-ps delay PTR^3 data is shown in Figure 5B. The several features which appear at 1475, 1260, 1171, 1124, and 1007 cm^{-1} can be reasonably correlated with RR bands recorded for the excited triplet state of β-carotene.[11,12,14,21] The difference spectrum obtained by subtracting 0.7 times the probe laser only RR spectrum from the 0-ps delay PTR^3 spectrum is presented in Figure 5A. Again, the several features which appear at 1478, 1172, 1124, and 1010 cm^{-1} are assignable to the excited triplet state of the carotenoids in *Ch. vinosum*. In addition, this spectrum also contains three features at 1524, 1240, and 1210 cm^{-1} which remain unassigned. Two other weak bands appear at 1608 and 1335 cm^{-1} and can be assigned to RR scattering from ground-state BChl.[37]

Discussion

The PTA and PTR^3 results presented here provide an improved understanding of the rates of singlet and triplet energy redistribution and of the molecular vibrations in electronically excited-state carotenoids during light-harvesting and photoprotective processes.

A. Absorption Data. The absorption changes occurring within the 8-ps excitation are assigned to a transition from the 2^1A_g state of the carotenoids on the basis of two experimental observations. First, PTA measurements performed on chromatophores which do not contain any carotenoids (i.e., blue green mutant of *Rhodobacter sphaeroides*) show only a decrease in sample absorbance at 590 nm which can be attributed to BChl.[40] This result is in contrast to the large absorbance increase in the 582–610-nm region shown in Figure 2. The increased carotenoid absorbance changes near 590 nm are apparently large enough to offset any decrease in sample absorbance due to the BChl in *Ch. vinosum*. Second, the increased sample absorbance observed at 582, 590, and 610

(37) Lutz, M.; Kleo, J. *Biochem. Biophys. Res. Commun.* **1976**, *69*, 711–717.
(38) Saito, S.; Tasumi, M.; Eugster, C. *J. Raman Spectrosc.* **1983**, *14*, 299–309.
(39) Iwata, K.; Hayashi, H.; Tasumi, M. *Biochim. Biophys. Acta* **1983**, *810*, 269–273.
(40) Hayashi, H.; Atkinson, G. H. Unpublished results.

nm (Figure 2) disappears at a rate (6.0 ± 0.5 ps) which is consistent with the decay lifetime of the carotenoid 2^1A_g state reported from studies of both isolated and chromatophore carotenoids.[17-20] The same decay time is measured here by PTA for all of the probe wavelengths at which the rapid (<8 ps) absorbance increase is observed (i.e., 582–650 nm). The 6.0 ± 0.5 ps decay time is about an order of magnitude slower than the estimated 1^1B_u state lifetime (<1 ps).[15,16] Thus, the transient absorption spectrum with a maximum near 620 nm (Figure 3A) is assigned to a $2^1A_g \rightarrow S_n$ transition of the carotenoids in *Ch. vinosum*. The upper state of this transition is not readily assigned. It is clear that the symmetry-allowed $2^1A_g \rightarrow 2^1B_u$ transition should be considered, but in the absence of a firm determination of the energetic position of the 2^1B_u state, such an assignment remains tentative.

The absorption spectrum of the $2^1A_g \rightarrow S_n$ transition can be readily separated by direct time resolution from longer lived absorption assigned to the $T_1 \rightarrow T_n$ transition. Both absorption transitions can be observed in Figure 3. The 2^1A_g state decays rapidly (6 ps) leaving only the absorption from the triplet carotenoids for delays longer than 18 ps. The remaining absorbance over the entire 573–650-nm region, therefore, can be assigned to the $T_1 \rightarrow T_n$ transition. Although this $T_1 \rightarrow T_n$ absorption decreased between 25 and 400 ps delays, it remains detectable for delays greater than 1 ns (data not shown in Figure 3). The precise shape of the $T_1 \rightarrow T_n$ spectrum cannot be obtained from the data presented in Figure 3, although it is evident that the spectral maximum lies at a wavelength less than 570 nm.

These PTA results are in good agreement with those reported on *Rs. rubrum* where absorption changes assignable to both carotenoids and BChl are measured after 532 nm, pulsed (35 ps) laser excitation.[17] The increased sample absorbance (maximum at 575 nm) observed after 200-ps time delay is assigned to the excited triplet state of the carotenoids. This carotenoid $T_1 \rightarrow T_n$ absorption spectrum correlated well with the results presented here including the appearance of a long spectral tail to the red of the absorption maximum. Only a small absorption feature near 610 nm, measured during the cross-correlation period, could be associated with the population of the excited singlet state of the carotenoids in the *Rs. rubrum* sample. Neither an assignment to a specific excited singlet state (i.e., 1^1B_u or 2^1A_g) nor a clear separation of the singlet versus triplet absorption was feasible given the 35-ps time resolution. The 8-ps time resolution of the PTA data presented here resolves both these issues for *Ch. vinosum*.

B. Vibrational Raman Data. The RR spectrum of T_1 state carotenoids can be obtained from the PTR^3 data presented in Figure 4 if the ground-state carotenoid contributions can be correctly measured and subtracted. In principle, the RR scattering from ground-state carotenoids is contained in the probe laser only spectrum shown as Figure 4A. The 4 mW power and 595 nm wavelength of the probe laser are selected purposefully to avoid photolytic perturbations which could result in forming excited-state carotenoid intermediates. By subtracting the probe laser only RR spectrum from the two laser, PTR^3 data recorded at a given time delay, the RR scattering due to the transient species present during that part of the reaction can be obtained. The principal unknown in this analysis is the factor appropriate for scaling the probe laser only RR spectrum. The initial scaling factors have been selected on the basis of an empirical criterion, namely to avoid obtaining RR bands with negative intensities in the resultant difference spectrum. Scaling factors of 0.65–0.75 for the 0-ps delay data and 0.98 for the 50-ps delay data are selected since the resultant difference spectra contain no significant intensity in the 1148-cm^{-1} ground-state carotenoid band (Figure 5). In addition, the 0.98 value for the scaling factor for the 50-ps delay data is supported by the PTA data, vide infra.

The mechanistic interpretation of the PTR^3 results is analogous to that used for the PTA data. The kinetic properties associated with optical pumping process (ground-state depletion and repopulation) and the formation and decay of the T_1 state both can be observed through the intensity changes of RR bands. Specifically, during optical pumping, the intensities of the 1148 and 1508 cm^{-1} RR bands assigned to the carotenoid ground state

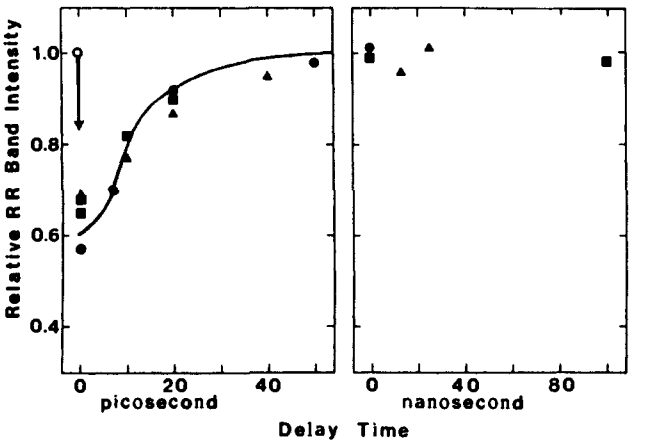

Figure 6. Time depencence of the intensities for the 1148-cm^{-1} RR band assigned to ground-state carotenoids. Band intensities are measured directly from PTR^3 spectra recorded with pump and probe laser wavelengths at 560 and 590 nm, respectively. The initial 1148-cm^{-1} band intensity is shown as an unfilled circle (○). Data from three different experiments (▲, ■, ●) are plotted together for two time scales. The initial two data points (■, ●) shown for the nanosecond time scale at the extreme left are recorded with a 100-ps delay. The solid line models the time dependence of a 6-ps decay convoluted with 8-ps pump and probe pulses and a 14-ps cross-correlation time.

decrease by 30% (Figure 4), reflecting the optical depopulation of the 1^1A_g state. These data suggest that a 0.70 scaling factor of the probe only RR spectrum correctly accounts for the ground-state contribution to the 0-ps delay PTR^3 data (Figure 5).

The kinetics associated with the recovery in intensity of the 1148 and 1508 cm^{-1} RR bands can be seen in Figure 6 where the 1148-cm^{-1} band intensities (measured as peak heights directly from PTR^3 spectra) are plotted versus delay times over two scales. The lifetime for recovery of the 1^1A_g population is about 6 ps which is in reasonable agreement with the 2^1A_g decay time measured by PTA vide supra. This agreement suggests that the principal relaxation processes underlying 1^1A_g repopulation involve the 2^1A_g state. These processes may include intramolecular internal conversion and energy-transfer processes involving either BChl or the T_1 state of the carotenoids.

Although the process involving the T_1 state of the carotenoids is considered to have a very small yield, it can be monitored directly by PTR^3 data. Several new RR bands assignable to T_1 carotenoids (at 1475, 1260, 1171, 1124, and 1007 cm^{-1}) are evident in the difference RR spectrum (Figure 5) and increase continuously in intensity until maxima are reached for delays of about 50 ps. The rate of increase is seen quantitatively when the relative intensity of the 1124-cm^{-1} band is plotted versus delay time (Figure 7). By deconvoluting the cross-correlation pulse width, the time constant at which this band reaches its maximum intensity can be approximated to be 6 ps. This lifetime parallels closely the decay time of the 2^1A_g state, thereby suggesting that the excited-state processes which lead to the formation of the T_1 state also involve the 2^1A_g state. The relaxation of the T_1 state over a 100-ns time period can be qualitatively monitored from the decreasing intensities of the 1125-cm^{-1} band (Figure 7). Although the intensity decrease is measured for only a relatively short period, the decay time of T_1 can be estimated to be approximately 250 ns.

A relatively simple, though only partially complete, model for excited-state processes in the *Ch. vinosum* carotenoids can be derived from these picosecond data (Figure 8). The optical population of the 1^1B_u state is followed by rapid (<1 ps) relaxation to the 2^1A_g state. The appearance of absorption from the 2^1A_g state within the cross-correlation time (~14 ps) of these measurements (Figures 2 and 3) is consistent with such rapid relaxation of the 1^1B_u population into the 2^1A_g state. It is from the 2^1A_g state that the transient absorption centered near 620 nm occurs. The repopulation rate of the 1^1A_g state, as monitored by the increasing intensity of the 1148 cm^{-1} RR band (Figure 6), is controlled by the decay of the 2^1A_g state, as monitored by the

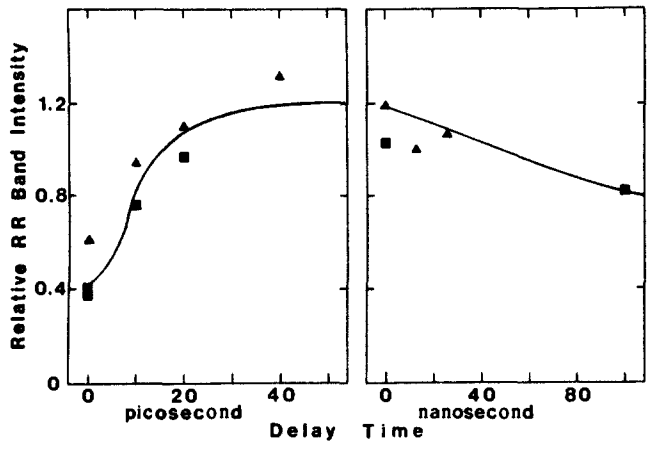

Figure 7. Time dependence of the intensities for the 1125-cm^{-1} RR band assigned to excited triplet state carotenoids. Band intensities are measured from difference RR spectra such as shown in Figure 5. Pump and probe laser wavelengths at 560 and 590 nm, respectively, are used. Data from two different experiments (■ and ▲) are plotted together for two time scales. The initial two data points (■ and ▲) shown for the nanosecond time scale at the extreme left are recorded with a 100-ps delay. For the picosecond time scale panel, the solid line models the time dependence of a 6-ps decay convoluted with 8-ps pump and probe pulses and a 14-ps cross-correlation time. In the nanosecond time scale panel, the data were fit with a nonlinear least-squares fit by using an $A \exp(-kt)$ decay function, yielding a 250-ns decay time constant.

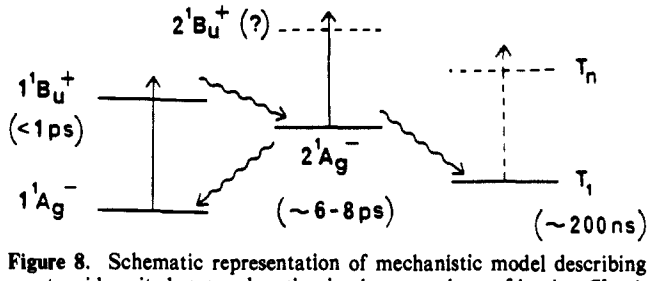

Figure 8. Schematic representation of mechanistic model describing carotenoid excited-state relaxation in chromatophore of in vivo *Ch. vinosum*.

decreasing intensity of the 620-nm absorption (Figure 3). Two molecular processes are of primary importance in the relaxation of 2^1A_g carotenoids: energy transfer to BChl [Car(2^1A_g) + BChl (S_0) → Car(1^1A_g) + BChl (S_1)] and internal conversion [Car(2^1A_g) → Car(1^1A_g)]. Both processes result in the formation of ground-(1^1A_g)state carotenoids and, therefore, essentially all of the excited-state carotenoid population should return to the 1^1A_g state. This anticipated result is confirmed in the PTR[3] data presented in Figure 6. The intensity of the 1148-cm^{-1} band returns to its original value after approximately 50 ps. The error bars for this measurement are about 2%. This result suggests that a 0.98 scaling factor of the probe laser only RR spectrum correctly accounts for the ground-state contribution to the 50-ps delay PTR[3] data (Figure 5).

This view of the molecular mechanism is supported by the 1^1A_g repopulation and 2^1A_g relaxation rates as obtained by two completely separate measurements (PTR[3] and PTA spectroscopy, respectively). These values also are consistent with measurements of ground-state repopulation in isolated carotenoids in organic solvent (e.g., 8.4 ps for β-carotene in toluene[19]) and singlet energy transfer in light-harvesting II antenna complexes of *Rhodobacter acidophila*.[20] The formation of the T_1 state also is dominated by the relaxation of the 2^1A_g state. This view is consistent with the proposal that fission between 2^1A_g and 1^1A_g state carotenoids is the major process by which two T_1 states are formed[23-26] although this process accounts for only a small percentage of the total 2^1A_g carotenoids undergoing decay. The agreement between the rates at which the T_1 state appears and the 2^1A_g state decays strongly supports this model.

The relative amount of T_1 carotenoid can be determined from the changes in absorbance measured in Figures 2 and 3 and the extinction coefficients extracted from data presented in Figure 5a of ref 17. The difference spectrum presented in ref 17 shows that the increase in absorbance due to the presence of triplet spirilloxanthin measured at 550 nm, monitoring the $T_1 \rightarrow T_n$ transition, is 2.5 times more intense than the $1^1A_g \rightarrow 1^1B_u$ transition at 470 nm. This yields a ϵ_{550} for the $T_1 \rightarrow T_n$ transition of 2.5 × 152 mM^{-1} cm^{-1} = 380 mM^{-1} cm^{-1} for carotenoids in chromatophores from *Ch. vinosum*. The extinction coefficient at 590 nm is approximately 1/3 of the extinction coefficient at 550. Taking the ΔA of 0.012 measured at 590 nm and the path length through the sample jet, 0.03 cm, the concentration of triplet carotenoid is 1 μM or about 1% of the sample. This 1% value supports the conclusions concerning the repopulation of the 1^1A_g state based on the 1148-cm^{-1} RR band intensities after 50 ps vide supra.

The ϵ value of the $2^1A_g \rightarrow S_n$ transition also can be estimated from the PTR[3] and PTA data. Since during optical pumping, the ground-state carotenoid population decreases by at least 30% (Figure 4) and the sample absorbance at 620 nm increases (ΔA = 0.03 with 300 μm pathlength) (Figure 3), the difference between the $1^1A_g \rightarrow 1^1B_u$ and $2^1A_g \rightarrow S_n$ values of ϵ can be calculated. With ϵ for $1^1A_g \rightarrow 1^1B_u$ equal to 152 mM^{-1} cm^{-1},[41,42] the ϵ for 2^1A_g is estimated to be 30 mM^{-1} cm^{-1}.

The time resolution underlying the PTA data presented here permits the observation of a previously unreported 80-ps transient absorption signal. Since this 80-ps decay process is observed for probe wavelengths throughout the 573–650 nm spectrum assigned to the $T_1 \rightarrow T_n$ transition, it is reasonable to conclude that it reflects the relaxation of at least part (~30%) of the T_1 carotenoid population. Such a process is distinct from the intersystem crossing to the 1^1A_g state which can be assigned to the longest decay rate (>200 ns) observed. The observation of two decay rates suggests that there are two distributions within the T_1 carotenoid population which relax separately.

Although the 80-ps component remains to be characterized fully, its tentative association with triplet–triplet (T_1–T_1) annihilation between closely spaced pairs of T_1 carotenoids is an instructive case to consider.[43,44] Such a process is analogous to the well-known S_1–S_1 annihilation reported for BChl in the light-harvesting antenna complexes of chromatophores.[45,46] Triplet–triplet annihilation would reduce the amount of T_1 carotenoid present in the chromatophores and be observed as an overall decrease in the 580–620 nm wavelength region. Alternative interpretations based on the decay of S_1 BChl via either energy trapping by the photosynthetic reaction centers in the chromatophores or S_1–T_1 fusion involving S_1 BChl and T_1 carotenoids[47-50] are in disagreement with the observed PTA results. In the case of S_1–T_1 fusion, excited S_1 state BChl interacts with triplet T_1 carotenoid to produce ground-state BChl and a higher energy excited triplet state of the carotenoid. Over the wavelength region studied, 580–620 nm, the ground-state BChl absorbance would recover as the result of S_1–T_1 fusion and the T_1 absorbance of the carotenoids would remain. As a result, the amplitude of the 80-ps component would increase in absorbance rather than the observed decrease. Singlet energy trapping by the reaction centers in the chromatophore membranes would also result in the recovery of the ground-state antenna BChl absorbance in the 580–620-nm region. In both of these cases, transient absorbance should increase

(41) Goedheer, J. C. *Biochim. Biophys. Acta* **1959**, *35*, 1-8.
(42) Thornber, J. P. *Biochemistry* **1970**, *9*, 2688-2698.
(43) Johnson, R. C.; Merrifield, R. E. *Phys. Rev. B* **1970**, *1*, 896-902.
(44) Frankevich, E. L.; Pristupa, A. I.; Lesin, V. I. *Chem. Phys. Lett.* **1977**, *47*, 304-308.
(45) Van Grondelle, R. *Biochim. Biophys. Acta* **1985**, *811*, 147-195.
(46) Campillo, A. J.; Hyer, R. C.; Monger, T. G.; Parson, W. W.; Shapiro, S. L. *Proc. Natl. Acta Sci. U.S.A.* **1977**, *74*, 1997-2001.
(47) Monger, T. G.; Parson, W. W. *Biochim. Biophys. Acta* **1977**, *460*, 393-46.
(48) Monger, T. G.; Cogdell, R. J.; Parson, W. W. *Biochim. Biophys. Acta* **1976**, *449*, 136-153.
(49) Mauzerall, D. *Biophys. J.* **1976**, *16*, 87-91.
(50) Campillo, A. J.; Kollman, V. M.; Shapiro, S. L. *Biophys. J.* **1976**, *16*, 93-97.

rather than decrease as is observed.

A T_1-T_1 annihilation mechanism also provides a basis for describing the two distributions in the T_1 carotenoid population. For T_1-T_1 annihilation to be an effective T_1 decay route, the T_1 molecules must be at or near van der Waals distances to each other. This distance restriction would seem to prohibit T_1-T_1 annihilation with a T_1 carotenoid concentration of only 1 μM or 1% of the total carotenoid population. However, it must be emphasized that the T_1 carotenoids are formed by singlet fission as adjacent triplet pairs, at van der Waals distances, and annihilation should simply be considered as the reverse reaction. Triplet formation would then be described with a <6 ps time constant and T_1-T_1 annihilation described by an approximately 80-ps time constant. Competitive with T_1-T_1 annihilation is rapid triplet energy transfer (i.e., triplet diffusion) that results in the separation of the triplet pairs from each other. These remaining T_1 carotenoids are then located far enough from one another to prevent T_1-T_1 annihilation and, consequently, relax via the slower, normal intersystem crossing mechanism. This interpretative model remains speculative, and further experimentation is required to more completely characterize the phenomenon.

Acknowledgment. The authors gratefully acknowledge the technical assistance of T. L. Brack. Partial support for this work was provided by a grant from the DuPont Corporation for the exchange of Japanese and American researchers. G.H.A. thanks the Alexander von Humboldt-Stiftung and Professor E. Schlag for their support and hospitality at the Technical University of Munich where part of this manuscript was prepared.

Registry No. Rhodopin, 105-92-0; spirilloxanthin, 34255-08-8.

^{89}Y MAS NMR Study of Rare-Earth Pyrochlores: Paramagnetic Shifts in the Solid State

Clare P. Grey,[†] Mark E. Smith,[‡] Anthony K. Cheetham,*[,†] Christopher M. Dobson,[§] and Ray Dupree[‡]

Contribution from the Chemical Crystallography Laboratory, University of Oxford, 9 Parks Road, Oxford OX1 3PD, U.K., Inorganic Chemistry Laboratory, University of Oxford, South Parks Road, Oxford OX1 3QR, U.K., and Physics Department, University of Warwick, Coventry CV4 7AL, U.K. *Received June 9, 1989*

Abstract: ^{89}Y MAS NMR spectra have been obtained from yttrium pyrochlores $Y_{2-y}Ln_yM_2O_7$ (Ln = Ce, Pr, Nd, Sm, Eu, Yb; M = Sn, Ti). Incorporation of the paramagnetic ions into the diamagnetic compounds was found to cause large reductions in the ^{89}Y nuclear relaxation times enabling spectra to be accumulated in relatively short times in comparison to similar diamagnetic systems. In addition to the resonances of the diamagnetic end-member compounds, $Y_2Sn_2O_7$ and $Y_2Ti_2O_7$, extra ^{89}Y resonances were observed, due to the substitution of paramagnetic ions into the local coordination sphere surrounding an ^{89}Y nucleus. The paramagnetic shifts were found to be proportional to the number of lanthanide ions substituted for yttrium in the first coordination sphere; the intensities of the resonances could be used to determine the concentration of paramagnetic rare-earth ions in the diamagnetic phase. The direction and magnitude of the shifts induced by the presence of paramagnetic ions suggest that there could be a significant contribution from a dipolar mechanism.

High-resolution solid-state NMR, using a wide variety of different nuclei, has proved to be of considerable value in studies of a wide range of both crystalline and amorphous inorganic materials. The many diverse applications have included the elucidation of structure, dynamics, and reaction mechanisms.[1] However, for many nuclei, despite their chemical importance, lack of resolution, low sensitivity, and long relaxation times can restrict the systems that can be studied and limit the information that can be obtained. One approach to assist in the study of such materials is to exploit some of the effects of incorporating paramagnetic ions into solids. The use of low concentrations of iron and manganese to reduce the relaxation times of ^{29}Si nuclei in glasses and cements is already established,[2,3] as is the use of copper to reduce the recycle delays in the magic angle spinning (MAS) NMR of biomolecules.[4] In general, however, paramagnetic ions have, as yet, been little exploited in the solid state, despite their widespread use as shift and relaxation probes in solution.[5-7] Paramagnetic lanthanides are particularly suitable for study since they all, except Gd^{3+}, have short electron relaxation times[6-8] and hence may not always cause excessive broadening of resonances in the NMR spectra. Indeed, it has recently become apparent that it is possible to both obtain and interpret high-resolution NMR spectra from solids containing paramagnetic lanthanides. In addition to ^{13}C MAS NMR studies of lanthanide acetates,[9,10] which are molecular structures, the applicability of MAS NMR to the study of paramagnetic continuous solids has been demonstrated,[11,12] particularly in probing local order in solid solutions. The latter studies, which used ^{119}Sn, yielded a dramatic increase

[†] Chemical Crystallography Laboratory, University of Oxford.
[‡] University of Warwick.
[§] Inorganic Chemistry Laboratory, University of Oxford.

(1) Fyfe, C. A. *Solid State NMR for Chemists*; C.F.C. Press: Guelph, Ontario, Canada, 1983; pp 6-7.
(2) Fujiu, T.; Ogino, M. *J. Non-Cryst. Solids* **1984**, *64*, 287-290. Dupree, R.; Holland, D.; McMillan, P. W.; Petifer, R. F. *J. Non-Cryst. Solids* **1984**, *68*, 399-410.
(3) Dobson, C. M.; Goberdhan, D. G. C.; Ramsey, J. D. F.; Rodger, S. A. *J. Mater. Sci.* **1988**, *23*, 4108-4114.
(4) Ganapathy, S.; Naito, A.; McDowell, C. A. *J. Am. Chem. Soc.* **1981**, *103*, 6011-6015.
(5) Hinckley, C. C. *J. Am. Chem. Soc.* **1969**, *91*, 5160-5162.
(6) Dobson, C. M.; Levine, B. A. *New Techniques in Biophysics and Cell Biology*; Pain, R. H., Smith, B. J., Eds.; Wiley-Interscience: New York, 1976; Vol. 3, pp 19-90.
(7) Inagaki, F.; Miyazawa, T. *Progress in NMR Spectroscopy*; Pergamon Press: New York, 1981; Vol. 14, pp 67-111.
(8) Alsaadi, B. M.; Rossotti, F. J. C.; Williams, R. J. P. *J. Chem. Soc., Dalton Trans.* **1980**, 2147-2150.
(9) Chacko, V. P.; Ganapathy, S.; Bryant, R. G. *J. Am. Chem. Soc.* **1983**, *105*, 5491-5492. Ganapathy, S.; Chacko, V. P.; Bryant, R. G.; Etter, M. C. *J. Am. Chem. Soc.* **1986**, *108*, 3159-3165.
(10) Campell, G. C.; Crosby, R. C.; Haw, J. F. *J. Magn. Reson.* **1986**, *69*, 191-195.
(11) Cheetham, A. K.; Dobson, C. M.; Grey, C. P.; Jakeman, R. J. B. *Nature (London)* **1987**, *328*, 706-707.
(12) Grey, C. P.; Dobson, C. M.; Cheetham, A. K.; Jakeman, R. J. B. *J. Am. Chem. Soc.* **1989**, *111*, 505-511.

0002-7863/90/1512-4670$02.50/0